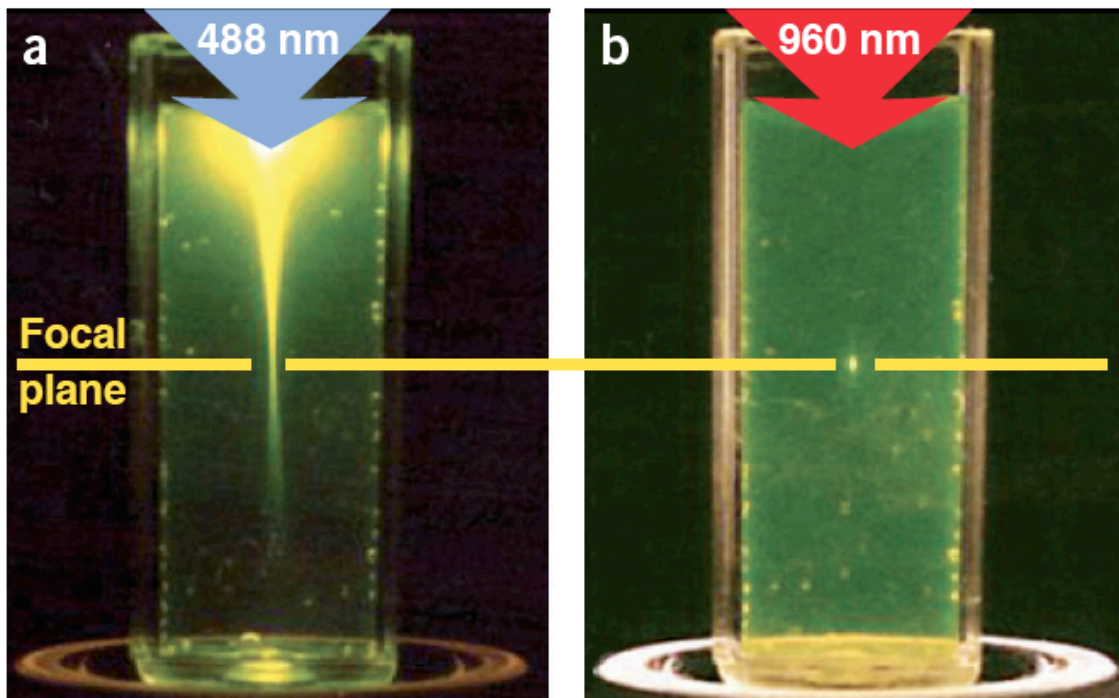


## Introduction:

Multi-photon microscopy (MPM) is a noninvasive method of fluorescence microscopy used in examining tissue sections and living animals. It has been used to study calcium dynamics in the brain<sup>1,2</sup>, neuronal plasticity<sup>3</sup>, cancer angiogenesis<sup>4,5</sup>, and lymphocyte trafficking<sup>6</sup>. It has also been used to measure cerebral blood flow (CBF)<sup>7</sup> and as a tool for cell cutting and ablation<sup>8</sup>.

Three-dimensionally localized excitation depends on two photons interacting with a molecule nearly simultaneously on the order of  $10^{-16}$  s. This results in the occurrence probability of two-photon excitation (TPE) having a quadratic dependence on light intensity<sup>9</sup>. This is in contrast to conventional fluorescence, which has a linear dependence on light intensity. Due to this quadratic dependence, TPE can be highly localized to a focal plane of choice as away from the focal plane, the TPE probability drops off rapidly (Fig. 1).

**Figure 1**<sup>9</sup>



However to make two-photon microscopy practical, the beam must be concentrated in both space and time. This will increase the probability of TPE and number of fluorescence photons generated for measurement. To concentrate the light in time, a pulse laser is used. This increases laser intensity while keeping the average power relatively low<sup>9</sup>. In our system, this is established with mode-locking, and is apparent when the measured frequency of the beam becomes less well-defined as the uncertainty principle dictates will occur with ultra-short pulses in time.

Two-photon scanning microscopy has advantages over conventional microscopy, which has limited spatial signal localization and major scattering of light in living tissues. Conventional microscopy is thus limited in its applications to cells in culture, sectioned tissues and select small organisms such as nematodes. TPE on the other hand has excellent spatial localization as noted above, and it is also associated with less light scattering since it uses photons of longer wavelength and lower frequency. This allows TPE to penetrate into deeper tissue with greater accuracy. This translates into the ability to make non-invasive measurements as deep as 500  $\mu\text{m}$  into living tissue whereas conventional fluorescence is limited to at least half of this<sup>10</sup>.

In addition, TPE does not generate out-of-focus fluorescence since its photon absorption is confined to a narrow region at the plane focus. Thus while conventional microscopy requires a pinhole to eliminate photons from out-of-focus areas, TPE does not require such a pinhole. This results in increased fluorescence collection efficiency over conventional microscopy, because scattered light emitted from an excited fluorophore can still be collected<sup>11</sup>. Finally, TPE also minimizes the occurrence of photobleaching and photodamage due to its ability to achieve high spatial localization<sup>12</sup>.

For this project, we explored our ability to build a two-photon microscopy system. Once the system was assembled, we used it to simulate measurements of blood flow using a capillary phantom. In addition, we tested its ability to perform cell ablation.

## Methods:

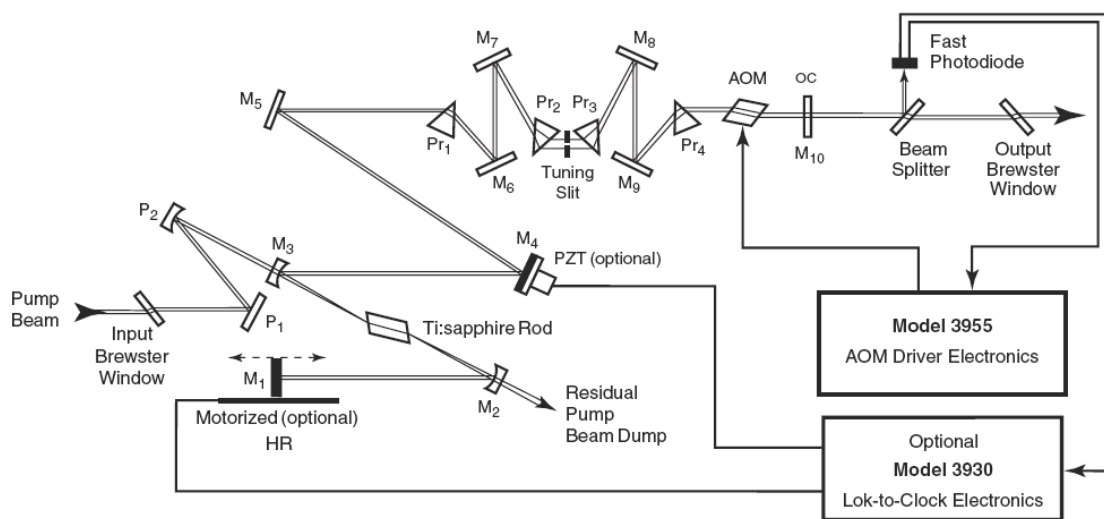
### *System Overview:*

Our 2-photon laser system consisted of a Millennium V CW Visible Laser, a Tsunami mode-locked Ti:sapphire Laser, spectrophotometer, power meter, gold mirrors, scanning mirrors, lens, a 220 focal length objective, a condenser, filter, photodiode, AC amplifier, and analog to digital converter (ADC).

### *Laser Alignment:*

The first consideration in building the two-photon laser was ensuring proper alignment of the Millennium and Tsunami lasers. To start the quarter, they were aligned but became misaligned due to user error. After reading through the manual, we determined that adjusting the beam steering mirrors  $P_1$  and  $P_2$  would fix the problem (Fig. 2).

**Figure 2**



Tsunami User's Manual (Spectra-Physics, June 2002)

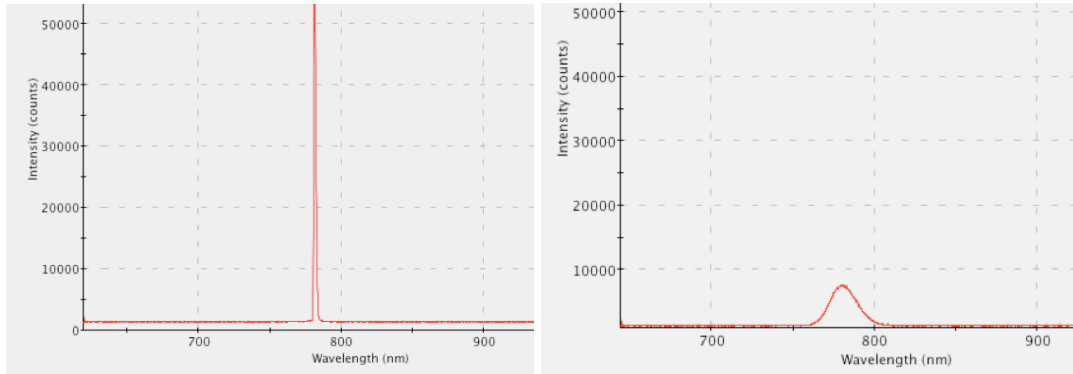
We performed fine-tuning of  $P_1$  and  $P_2$  by ensuring the beam projection onto mirror  $M_4$  did not have astigmatism or different foci in its two perpendicular planes. We also adjusted the tuning slit to improve beam intensity while maintaining the ability to mode-lock the laser.

### *Beam Characteristics:*

Mode-locking is a critical ability of the two-photon system. It produces ultra-short laser pulses that concentrate beam intensity in a very brief amount of time. This increases the probability that two photons will interact to produce fluorescence. To achieve mode-locking, we adjusted the prism dispersion compensation control and less often we adjusted the output coupler ( $M_{10}$ ) and the high reflector ( $M_1$ ). When mode-locking is

achieved, the uncertainty principle dictates that the ultra-short pulses will result in decreased ability to accurately determine the frequency (Fig. 3).

**Figure 3:**



We determined the beam intensity to be 0.49W using a power meter and the wavelength to be about 780 nm using a spectrophotometer.

Using gold mirrors, we routed the beam to an optical track with scanning mirrors, lens and a filter and photodiode for detection. Details of the scanning mirror are below. We used a lens with focal length of 76.2 mm to focus the beam on a 210 mm objective. We mounted the blood flow phantom on a condenser ( $f=50$  mm) in order to maximize the number of emitted photons collected. We placed an additional 50 mm lens to move the focal point closer, and placed a filter with a transmission greatest in the 340-600 nm range.

To maximize the power of the laser while keep the laser tightly focused on the sample, we must correctly fill the back aperture of the objective. The beam width of the laser is necessary to calculate the expanding factor and the parameters necessary in order to achieve this. Usually the profile of a laser beam is a 2-D Gaussian function. Assuming the beam is circularly symmetric, either the full width at half maximum (HMFW) or two standard deviations ( $2s$ ) of the Gaussian function could be used as its effective beam width. Here we use the definition of  $2s$ .

To accurately measure the beam width, we followed these steps:

- Mounted a sharp-edged razor on a base whose position can be accurately controlled (**Fig. 4**)
- Put this mounted razor in between the laser beam and a power meter
- Slowly moved the razor from not blocking the laser at all to completely blocking the laser
- Recorded the position of the razor and the power of the laser on the power meter (**Fig. 5A**)
- Took the first order difference of the measured curve to get the beam profile
- Fitted the beam profile to Gaussian function (**Fig. 5B**)

**Figure 4:**



using 2s as its beam width.

Measured and fitted data is shown (**Fig. 5**). Effective diameter is 2.1mm.

**Figure 5:**

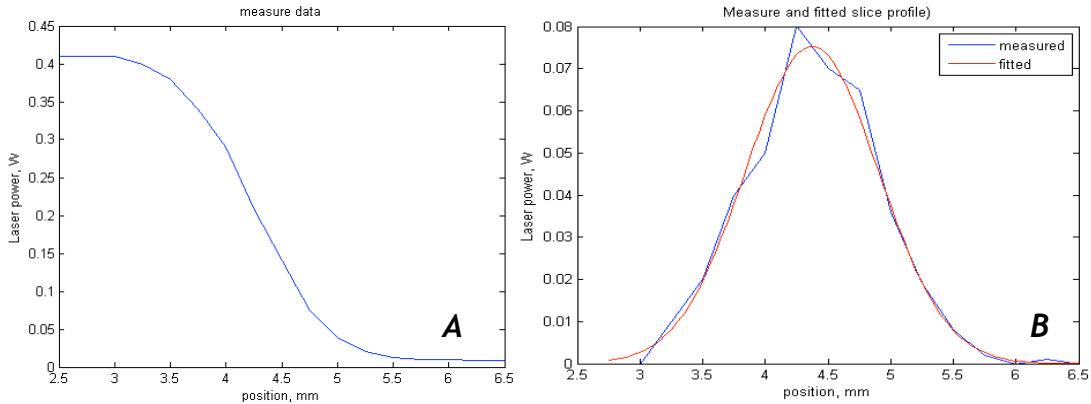


**Fig. 5A.** Measured laser power at different positions, **5B.** measured and fitted laser beam profile

#### *Raster Scanning:*

Two-photon fluorescence is a very location specific event. Therefore, it is necessary to scan the focused laser over the entire target to ensure that a proper image is recorded, not just at one focal length. The most common method used, and the one that we chose, is to scan the focal point of the converging laser by use of fast scanning mirrors.

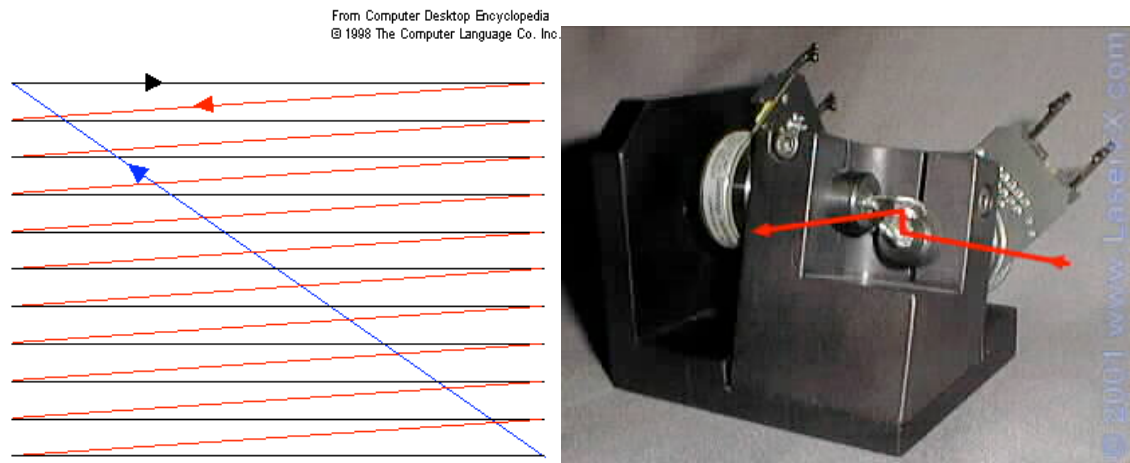
To our optical setup, we added a two-mirror fast scanning mirror (FSM) platform. The first mirror redirected the incoming laser light upwards, and the second mirror then sent it perpendicular to the original direction. The setup involved several lab periods of re-positioning and adjusting the gold mirrors located before the FSM since the angle at which the laser light entered the apparatus greatly affected the range and direction over which the light leaving the FSM could be adjusted. It was necessary to turn on the FSM before each adjustment since this system had a programmed zero-point. Turning on the system after adjustment would have resulted in a different optical path.

The directing of the laser path was subject to a few constraints, which made the task more difficult than expected. Primarily by using a 2-mirror system instead of a one-mirror device, the optical components before the FSM had to be removed, re-positioned, and re-adjusted. A one-mirror FSM allows for a single mirror to be computer controlled to tilt up and down, left to right, and any angle in between. The key advantage is that the mirror can simply be placed along the predefined optical axis, and then rotated for proper adjustment just as any regular redirection mirror is used. With the two-mirror system, the incoming beam is sent upwards which means that the optical axis before the FSM has to be lowered, or the axis afterwards has to be raised (since the non-FSM components were defined to the same axis before the addition of the FSM). Another difficulty is that any

deviation from the optimal approach angle sends the outgoing beam in a vertically diagonal direction, eventually raising the beam higher than the following components. The most difficult aspect however was the very small size of the 2 mirrors. It was not possible to simply tune the direction of the incoming light by adjusting the angle of the positioning mirrors, since only a very small amount of this could occur before the beam clipped the edge of the a mirror (resulting in loss of power and beam profile).

After final adjustments and redefining of the optical axis, the beam was refined with two lenses to ensure that the imaging conditions were ideal for our specific objective and that all light leaving the mirrors would enter the aperture. It was then necessary to add a computer controlled Rastor scanning pattern. This pattern is illustrated (**Fig. 6**), and is **very popular for laser microscopy and** imaging. The basic idea is to scan the laser over the target “one line at a time.”

**Figure 6:**



We used Matlab to control the scanning mirrors as they rotated to the appropriate angles for scanning across the sample. The mirrors require an analog controlling signal, so we used the data acquisition unit USB 1408-fs (see electronics part below) to convert the digital controlling signal to analog.

The maximum scanning speed of the mirrors is 80 Hz, and we need to send the controlling signal to both the motors that move the mirrors. Thus the total time to collect an image with a resolution of 32\*32 is  $2*32*32/80 = 25.6$  s. With this scanning rate of 25.6s/frame, we cannot capture simulated blood flow with reasonable resolution. We have to either lower the resolution or “freeze” the flow and then take images. In this project, we choose the latter (see results).

*Electronics:*

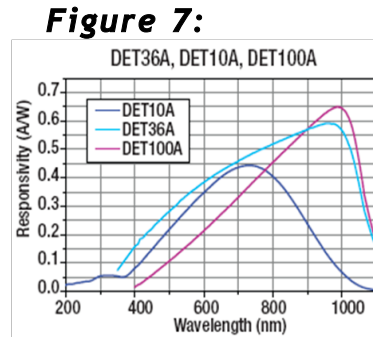
**In this project, we are using epi-collection mode. Therefore** once the fluorescent light is emitted, we need to filter out the **excitation light while** focusing as much of

the fluorescent light as possible on to **the detector**, a photodiode (DET100A Thorlabs). Though **the photodiode's** response (**Fig. 7**) is not optimized for this measurement (the emitted light has peak wavelength 521 nm), it is sufficient in our application when using combined with an amplifier.

Since the emitted light is very dim **and the photodiode's response is not optimal, the output current is very weak. Therefore, we used an amplifier built in-house to improve** detection of the fluorescent light by amplifying the current to voltage signal **by the** ratio 100 nA -> 1 Volt. **Unfortunately** this piece of amplifier compromised amplification at low frequencies, which affected our results, and will be addressed in results and discussion sections.

**Output of the amplifier is an analog signal, however data recording and storing equipment is digital. We used an ADC (USB 1408-fs, Fig. 8) to convert this signal from analog to digital for collection on our computer using a** Matlab function from toolbox daq to record the data (pin 1 as input channel 0 and pin 6 as analog ground). **Note this** same unit is used to send signals to control the scanning mirrors (pin 13, 14 as DAC output 1 and 2, pin 15 as analog ground).

**Figure 8:** our



### **Second Harmonic Generation (SHG):**

**Using a BBO crystal, which lacks inversion symmetry critical for SHG. The crystal location is very important due to this lack of inversion symmetry and required precise variation in the horizontal and vertical angle of the crystal, rotating it** perpendicular to the laser path through all possible values, and **adjustment of** the distance to the objectives **focal length. When this did not produce the desired result, we tried mounting the crystal to allow for micrometer adjustments and added an iris to trim the outer portions of the beam. This still did not produce the desired results, so finally we changed the objective, and this produced the desired image.**

### **Simulating Blood Flow Measurements:**

Our goal was to simulate blood flow measurement, so we built a “capillary” phantom. The “vessel” was a cylindrical straight glass tube with diameter about 500  $\mu\text{m}$ . We filled this tube with fluorescent solution containing 10 mM FITC (Fluorescein isothiocyanate), which has an excitation peak at 494nm and emission peak at 521nm. This simulated

“plasma,” and we mixed this with transparent spherical beads of diameter 350 - 400 um to simulate “red blood cells” moving in a capillary.

### ***Control of Scanning Pattern:***

***Since the purpose of our project was to measure the blood flow, we required the ability to acquire both spatial (displacement of beads) and temporal (the time point at measurement) information. Thus, we matched the scanning pattern to the purpose of our measurement.***

First, to improve the temporal resolution, we put the fast raster direction along the flow direction. ***To measure 1-D velocity as in this experiment, we scanned a single line at each time point, and stack all the lines as done by Kleinfeld et al. (1998). If 2-D velocity or structural information is need, one would have to do planar imaging, and the scanning speed would need to be fast enough to capture the flow.***

As mentioned in “Control scanning mirror with Matlab” section, the scanning speed is too slow to capture “real flow”, and it is not easy for us to pump the solution at a slow enough velocity to simulate the blood flow. So instead of reducing the resolution to do 1-D scan, we “froze” the motion of the flow, ***and simulated movement by blowing some air into the tube to move the beads. Therefore instead of measuring flow, we actually measured displacement. One of the advantages of this is that we can acquire more than one frame at each position and take the average to improve the SNR. In this experiment, we collected four frames and averaged to produce the final image. Since our field of view (FOV) is relatively small (about 150um \* 150um) compared to the object we are observing, we have to focus the FOV near the edges of the bead under examination. We then moved the bead to visualize the other edge in the FOV and repeated image acquisition.***

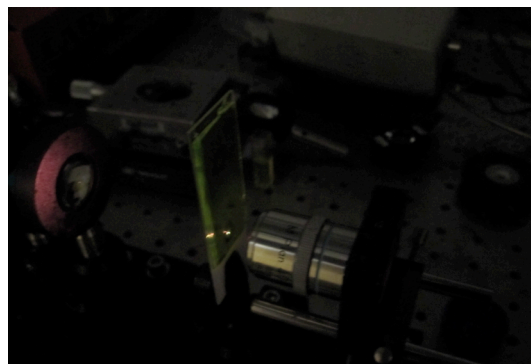
### ***Ablation:***

***The idea of adding ablation to the system was a side goal of the project, and was envisioned as using more of an upright microscope apparatus. However, we chose to add ablation to this system as a good pursuit of scientific curiosity. There were a few tasks to consider in adding ablation to the system. First, the scanning pattern of the FSM would need to be nullified to ensure that all available energy was focused at a single point and not spread around the sample.***

***This involved simply quitting the***

***Matlab program, but also meant that all targeting would have to be done manually by moving the sample throughout the fixed focal point.***

**Figure 9:**



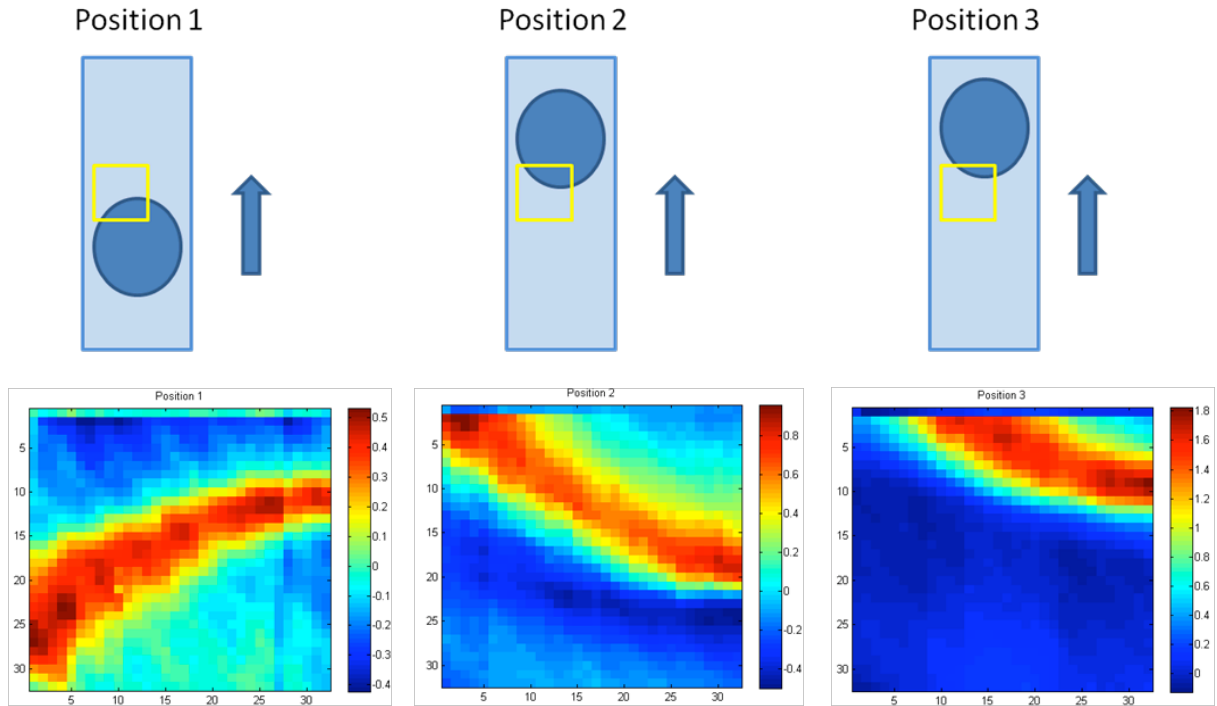
*The near full power of the system was used, which was about 4.8 mW, to ensure that the energy was sufficient to affect the target sample. This sample was a block of agarose gel, which was infused with fluorescein after learning that clear gel is very difficult to both target and image with a microscope afterwards. Since there was no microscope or imaging system before ablation, targeting relied on the addition of fluorescein. The target point was then seen as the point at which 2-photon fluorescence was produced (Fig 9).*

## Results

### Flow measurement:

The resulting **images** at different positions showed that the motion of the target bead was clearly imaged. One interesting **observation** is that the detection **only** seems **to be** sensitive to the **rapid** change of the **intensity of the fluorescence** where it occurred on the edges of the bead. **We also noticed that even using the average of 4 frames, we still observed some noise in the images, especially** at position 1 (**Fig. 10**).

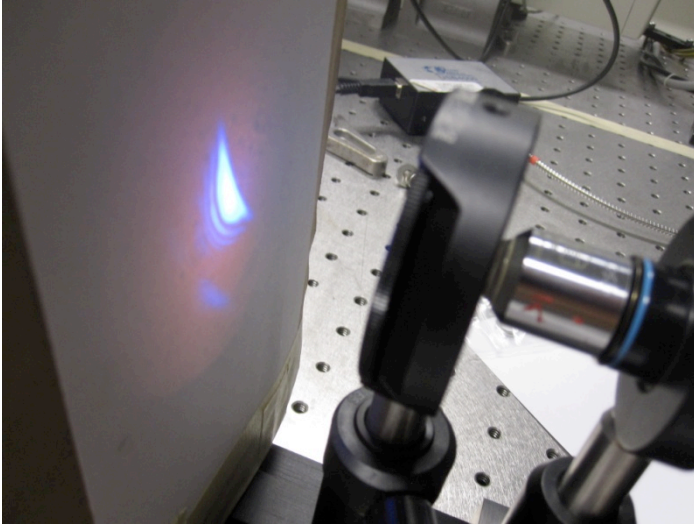
**Figure 10:** 2-photon scanning images after moving the target bead to different positions



*Second Harmonic Generation (SHG):*

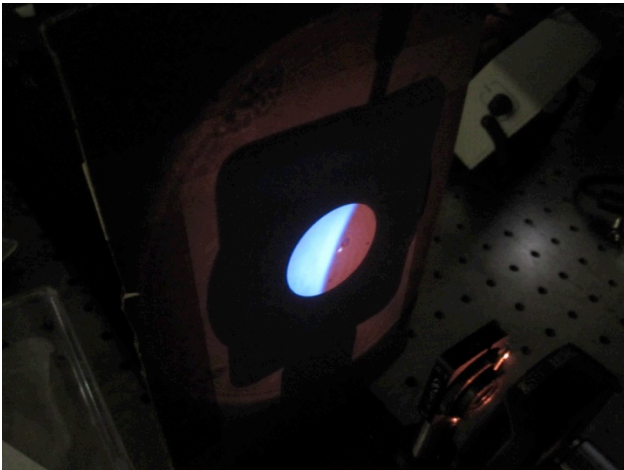
*Figure 11 shows our first observation of SHG. It is limited to half the light, and a clear aberration in the expected circular pattern is visible.*

**Figure 11:**



*After mounting the crystal to allow for micrometer adjustments and adding an iris to trim the outer portions of the beam, we found significant improvement in the shape of the image, however the crystal still only converted half of the light. (Fig 12).*

**Figure 12:**



*After we changed the objective, we finally produced the desired SHG image (Fig. 13).*

**Figure 13:**



*Ablation: The ablation was successful as shown by the light yellow spots (Fig. 14B),*

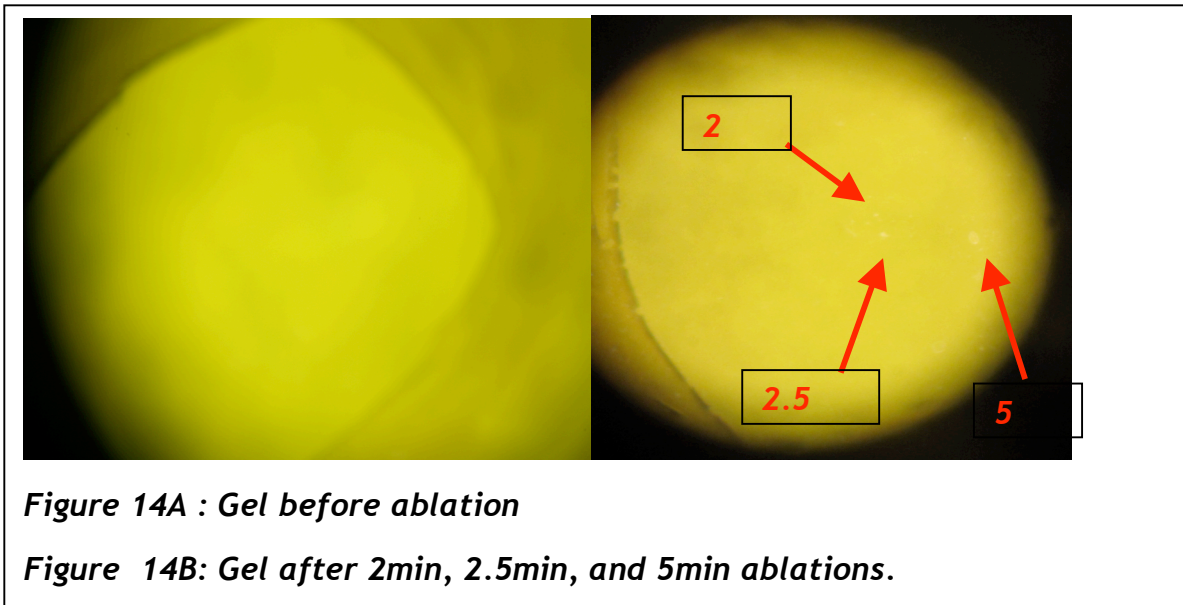


*Figure 14A : Gel before ablation*

*Figure 14B: Gel after 2min, 2.5min, and 5min ablations.*

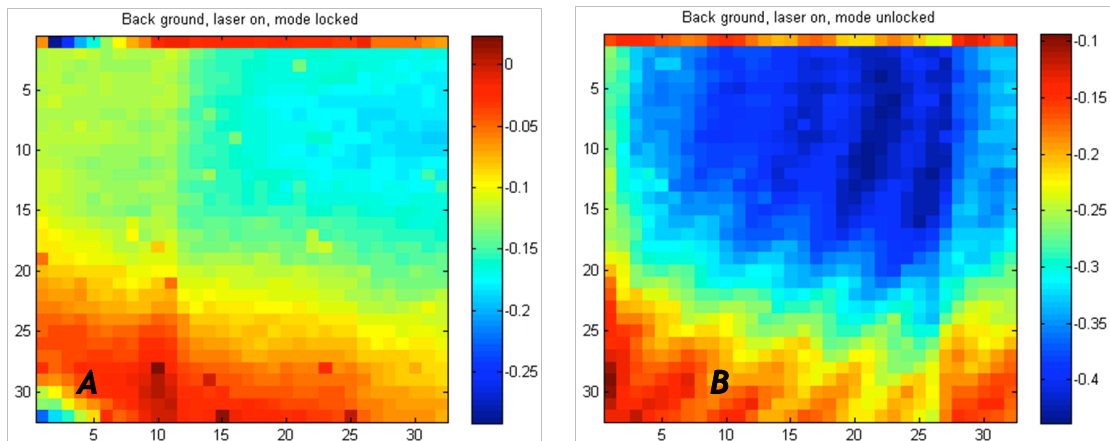
## **Discussion:**

### ***Measuring flow:***

***As mentioned in the “controlling scanning pattern” section, our measurement of flow was limited by the speed of the scanning mirrors compared to the flow velocity. Thus, we actually measured displacement rather than flow. If the scanning speed were faster or if we could simulate slow enough flow within the tube, then we would have been able to actually measure simulated blood flow.***

***Because of the amplifier compromised amplification at low frequency (DC component), it can be considered as an all-pass amplifier combined with a low-pass filter. This could be the reason why only the edge of the bead was detected while the signal both inside and outside the bead was low. This was also confirmed by taking images with only fluorescent fluid with mode-locking and without mode-locking as control (Fig. 15). This shows the signal difference is very small compared with the signal when edges are present.***

**Figure 15:** scanning images with (A) and without (B) mode locking



***The sensitivity to the intensity change instead of intensity itself could be either good or bad. The good thing is that it could be used to detect edges or sudden small movement of the object, which may not easily be detected on the intensity images. The bad thing is that it cannot tell if the scanning region is on the target or in the surrounding medium. To solve this problem, an amplifier with proper amplification at low frequency range could be used.***

***To reduce the noise of the data, we could have taken more frames and used the average, however, in a real flow measurement this would greatly reduce the temporal resolution. A better way to address this***

***problem would be to place a low pass filter after the amplifier to filter out the high frequency noise.***

### *Second Harmonic Generation:*

One of the goals of building the nonlinear optics system was to generate a beam of second harmonic light from outside components (not part of the manufactured laser). Since the Nd:YVO laser came with built in second harmonic generation, and the Ti Sapphire laser did not, we found it ideal to attempt second harmonic generation using the latter. The theoretical idea was to simply pass the laser light through a special crystal, which would cause a small fraction of the transmitted light to be frequency doubled (we would block the rest with a filter). In practice though, this proved to be a difficult task because of several factors.

The first of these factors was alignment through the crystal. The crystal used was a BBO crystal, which lacked inversion symmetry (critical for SHG). This lack of symmetry accounted for much difficulty in aligning the laser path, since even the slightest diversion from the optimum path resulted in the loss of 2<sup>nd</sup> harmonic generation. The initial installation onto the main rail resulted in no SHG ***phenomenon, and*** much time was spent varying the placement and approach angle of the laser light. After no success, the crystal was removed and examined under a microscope for defect. It was then re-mounted and every angle possible ***as detailed in the methods section.*** This first lack of generation came with the acknowledgement that the working distance of our objective was too short to actually reach the plane of the crystal, which was mounted a few mm inside of a thick ring holder. Thus, the objective was changed to one with a longer working distance, and the entire process was repeated, with no success. After further examination, we determined that the center of the crystal had been shifted so that it was not sitting in the exact middle of the holder ring. Fine adjustments were carefully made to bring the center of the crystal to the center of the holder ring. This resulted in the first observation of second harmonic generation (***Fig. 9***). The blue light in the image represents the second harmonic (frequency doubled) light, and a clear aberration in the expected cylindrical pattern is visible.

After repeating the above process several times in an attempt to correct this pattern, we concluded that the problem was the lack of control over the depth of the crystal at which the focal plane was located. Again, because of lack of symmetry, and since the plane of the crystal is only a fraction of a ***millimeter*** thick (like a very thin glass window), a slight deviation from the center of the crystal can result in aberrations or loss of generation. To solve this problem we installed a mount, which had ***very fine micrometer adjustments; this allowed*** precise control and the ability to hit the center depth of the crystal. We also added a small iris to trim the outer portions of the beam, which may have contained non-desirable wavelengths. The result of ***these***

**modifications is shown (Fig. 10). Since** only half of the light **was frequency doubled (390nm)** and the other half to be unaffected (780nm), **there was still a problem**. After several rounds of changing lenses, angles, and adding various components (ie: waveplates) to fix this problem, it was agreed to try a different objective.

This proved to be a good decision, since the desired SHG phenomenon was produced immediately and with the expected cylindrical pattern. In retrospect, it is most likely that the two objectives we used previously contained some sort of internal half phase filter. This would account for why only half of the laser light generated the 2<sup>nd</sup> harmonic.

#### *Ablation:*

The agarose gel was not the optimal target for our ablation system because it had a few undesirable qualities. It was uniform in both structure and color, so imaging after the ablation was not as simple or clear-cut as looking for a specific ‘destroyed structure’ within a cell or other diverse sample. Also, the composition of a gel-like structure allows for the material to reform over any deformity, similar to how gelatin collapses in and reforms after puncturing with a finger. To overcome these issues, we used high ablation energy by setting the ablation to 2, 2.5, and five minutes respectively.

Imaging of the target sample was done before and after ablation using a 5X objective with a light microscope and recorded with a digital camera. This also provided some added difficulty in recording results, since it is very hard to represent what is seen in the microscope with a two-dimensional image with no contrasting colors or structures. However, the ablation was evident under the scope and the best images taken before and after are displayed.

## References

1. Yuste, R. & Denk, W. Dendritic spines as basic functional units of neuronal integration. *Nature* 375, 682-684 (1995).
2. Stosiek, C., Garaschuk, O., Holthoff, K., & Konnerth, A. In vivo two-photon calcium imaging of neuronal networks. *Proc. Natl. Acad. Sci. USA* 100, 7319-7324 (2003).
3. Svoboda, K., Tank, D.W., & Denk, W. Direct measurement of coupling between dendritic spines and shafts. *Science* 272, 716-719 (1996).
4. Brown, E.B. et al. In vivo measurement of gene expression, angiogenesis and physiological function in tumors using multiphoton laser scanning microscopy. *Nat. Med.* 7, 864-868 (2001).
5. McDonald, D.M. & Choyke, P.L. Imaging of angiogenesis from microscope to clinic. *Nat. Med.* 9, 713-725 (2003).
6. Cahalan, M.D., Parker, I., Wei, S.H. & Miller, M.J. Two-photon tissue imaging: seeing the immune system in a fresh light. *Nat. Rev. Immunol.* 2, 872-880 (2002).
7. Devor, A., Tian, P., Nishimura, N., Teng, I.C., Hillman, E.M.C., Narayanan, S.N., Ulbert, I., Boas, D.A., Kleinfeld, D., & Dale, A.M. Suppressed neuronal activity and concurrent arteriolar vasoconstriction may explain negative blood oxygenation level-dependent signal.
8. Tirlapur, U.K. & Konig, K. Targeted transfection by femtosecond laser. *Nature* 418, 290-291 (2002).
9. Zipfel, W.R., Williams, R.M., & Webb, W.W. Nonlinear magic: multiphoton microscopy in the biosciences. *Nat. Biotechnol.* 21, 1369-1377 (2003).
10. Centonze, V.E. & White, J.G. Multiphoton excitation provides optical sections from deeper within scattering specimens than confocal imaging. *Biophys. J.* 75, 2015-2024 (1998).
11. Oheim, M., Beaupaire, E., Chaigneau, E., Mertz, J. & Charpak, S. Two-photon microscopy in brain tissue: parameters influencing the imaging depth. *J. Neurosci. Methods* 111, 29-37 (2001).
12. Denk, W., Strickler, J.H. & Webb, W.W. Two-photon laser scanning fluorescence microscopy. *Science* 248, 73-76 (1990).
13. ***Kleinfeld, D., Mitra, P.P., Helmchen F., Denk, W. Proc. Natl. Acad. Sci. USA Vol. 95, pp. 15741-15746. (1998)***